Airframe Noise Reduction Technologies Applied to High-Lift Devices of Future Green Regional Aircraft

M. Barbarino, I. Dimino, A. Carozza, C. Nae, C. Stoica, V. Pricop, S.H. Peng, P. Eliasson, O. Grundestam, L. Tysell, et al.

▶ **To cite this version:**

M. Barbarino, I. Dimino, A. Carozza, C. Nae, C. Stoica, et al.. Airframe Noise Reduction Technologies Applied to High-Lift Devices of Future Green Regional Aircraft. 3AF / CEAS Conference "Greener Aviation: Clean Sky breakthroughs and worldwide status", Mar 2014, BRUXELLES, Belgium. hal-01082154

HAL Id: hal-01082154
https://hal.science/hal-01082154

Submitted on 12 Nov 2014

HAL is a multi-disciplinary open access archive for the deposit and dissemination of scientific research documents, whether they are published or not. The documents may come from teaching and research institutions in France or abroad, or from public or private research centers.

L'archive ouverte pluridisciplinaire **HAL**, est destinée au dépôt et à la diffusion de documents scientifiques de niveau recherche, publiés ou non, émanant des établissements d'enseignement et de recherche français ou étrangers, des laboratoires publics ou privés.

Executive Secretariat
6 Rue Galilée
75016 PARIS
Phone : 33 (0) 1 56 64 12 35
Fax : 33 (0) 1 56 64 12 31
E-mail : alexa.faucher@aaaf.asso.fr

AIRFRAME NOISE REDUCTION TECHNOLOGIES APPLIED TO HIGH-LIFT DEVICES OF FUTURE GREEN REGIONAL AIRCRAFT

M. Barbarino[1], I. Dimino[1], A. Carozza[1]

C. Nae[2], C. Stoica[2], V. Pricop[2]

S.-H. Peng[3], P. Eliasson[3], O. Grundestam[3], L. Tysell[3]

L. Davidson[4], L.-E. Eriksson[4], H.-D. Yao[4]

S. Ben Khelil[5], F. Moens[5], T. Le Garrec[5], D.-C. Mincu[5], F. Simon[5], E. Manoha[5], J.-L. Godard[5]

M. A. Averardo[6]

1. CIRA, Italian Aerospace Research Center, Italy
m.barbarino@cira.it; i.dimino@cira.it; a.carozza@cira.it

2. INCAS, National Institute for Aerospace Research "Elie Carafoli", Romania
cstoica@incas.ro; cnae@incas.ro; vpricop@incas.ro

3. FOI, Swedish Defence Research Agency, Sweden
peng@foi.se; peter.eliasson@foi.se; olof.grundestam@foi.se; lars.tysell@foi.se

4. Chalmers University of Technology, Sweden
lars.davidson@chalmers.se; lars-erik.eriksson@chalmers.se; huadong@chalmers.se

5. ONERA, The French Aerospace Lab, France
Saloua.Ben_Khelil@onera.fr; Thomas.Le_Garrec@onera.fr; Daniel-Ciprian.Mincu@onera.fr; frank.simon@onera.fr; eric.manoha@onera.fr; Jean-luc.godard@onera.fr

6. Alenia Aermacchi, Italy
michele.averardo@alenia.it

I. INTRODUCTION

Regional aircraft typically operate over airports located in the neighbourhood of densely populated areas, with high frequency of take-off / landing events and, hence, they strongly contribute to community noise and gaseous emissions. These issues currently limit further growth of traffic operated by regional airliners which, in the next future, will have to face even more stringent environmental constraints worldwide as prescribed by the civil aviation certification normative and local regulations as well.

Therefore, in accordance with ACARE Vision 2020 toward a drastic reduction of air transport environmental impact over next decades, several mainstream technologies have been considered in the frame of Clean Sky JTI – Green Regional Aircraft (GRA) ITD project for application to next-generation regional aircraft. Such technologies are concerning: i) advanced aerodynamics and load control to maximise lift-to-drag ratio in both design and off-design conditions of the whole flight mission profile, thus reducing fuel consumption/air pollutants emission and also allowing for steeper/noise-abatement initial climb paths; ii) load alleviation to avoid loads from gust encounter and manoeuvre exceeding given limits, thus optimising the wing structural design for weight saving; iii) low airframe noise to reduce aircraft acoustic impact in approach flight condition.

High-Lift-Devices (HLD) in fully-deployed settings represents one of the main sources of aircraft community noise during the approach flight phase and of consequent annoyance perceived by the resident population in the vicinity of airports. Therefore, in the overall scenario as above outlined, several HLD architectures, integrating either matured or more advanced low-noise concepts/technical solutions still preserving high-lift performances, have been investigated in the frame of the GRA ITD project. These HLD have been tailored to different classes/ configurations of future regional aircraft, ranging from high-wing 90-seat Turboprop to low-wing 130-seat Turbofan with different power-plant and engine installation.

Specifically, some passive acoustic devices have been numerically explored by the GRA partners by using different concepts and methodologies for Turbo-Prop (TP) and Open-Rotor (OR) AirCraft (A/C). The linedflap concept, the slat acoustic liner and the side-edge fences have been investigated and the main relevant results are respectively described in *Section II*, *III* and *IV*.

Furthermore, acoustically optimized High Lift Devices (HLD) have been studied. The multiobjective optimization of the high lift slat settings is described in *Section V* as well as the aerodynamic/acoustic assessment of conceptual HLD technologies in *Section VI*.

Finally, the experimental characterization of liners for the slat acoustic liner design and the experimental investigation of some of the described promising High-Lift Low-Noise technologies are respectively showed in the *Section VII* and *VIII*.

The main conclusions of the present paper are finally drawn in *Section IX*.

II. TP A/C WING LINEDFLAP CONCEPT

A passive noise reduction concept called lined-flap has been proposed and analysed by CIRA for a two-component wing of a Turbo-Prop Regional AirCraft [1]. The main idea of the linedflap was to conceive the flap as a multilayer liner with micro-perforation on the external facesheet as depicted in Figure 1.

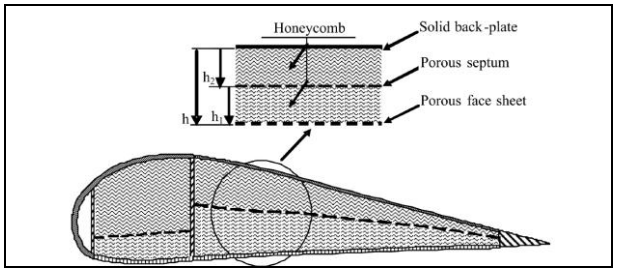

Figure 1: Schematic view of the linedflap concept.

A computational process has been essembled to design the linflap at the aim of defining an optimal impedance through the constructive parameters of the liner.

CFD and CAA computations have been performed for a twodimensional airfoil extracted from the wing section by requiring that the 2D wing profile operates at the same lift coefficient as the corresponding 3D wing section.

The threedimensional acoustic effects were roughly restablished by adding the quantity $10\log10(CLM/2\pi)$ to the computed 2D sound pressure levels (Ewert et al. [2]), accounting for the geometrical spreading of the acoustic energy and the statistical correlation of the noise sources in the spanwise direction. C is an empirical spanwise correlation parameter that relates the spanwise correlation length to the freestream velocity and frequency, L is the wingspan, R is the radiation distance, and M is the freestream Mach number.

In a first step, a CFD RANS simulation has been performed by using the commercial CFD software FLUENT.

The CFD boundary-layer properties in proximity of the trailing edge have been used to compute the magnitude of the wall-pressure Fourier components in a thin strip close to the main-wing trailing edge estimated through a semi-empirical model of the wall-pressure spectrum [4]. The wall-pressure Fourier components have been finally used as boundary condition of an acoustic FEM discretization.

In a second step, the acoustic field has been propagated through the mean flow and radiated to the far field over a prescribed frequency range by solving a homogeneous Howe's equation through a twodimensional finite element model (FEM) [3]. A user-defined function (UDF) Dirichlet boundary condition for the acoustic pressure has been used to set the value of the semi-empirical wall-pressure Fourier components at the trailing edge.

The effect of the acoustic treatment has been taken into account using Myers's boundary condition [5]. The value of the impedance on the flap surface has been computed through a combined analytical/semiempirical formula for a two degree of freedom (2-DOF) liner implemented as a UDF impedance boundary condition.

The value of the impedance of an acoustic treatment depends on the constructive properties of the liner and on the grazing flow conditions. Only semi-empirical models are available in the literature that allow to estimate the value of the impedance for given liner and flow properties, e.g., boundary-layer momentum thickness and asymptotic Mach number. The standard semi-empirical model reported in [6] for a 2-DOF liner filled with honeycomb has been used at the aim of estimating the liner impedance model, and quantifying

the noise reduction associated with the acoustic treatment.

The FEM code has been embedded in the environment of the commercial software Optimus [7], developed by Noesis Solutions, to compute the average overall sound pressure level (OASPL) over a radiation arc of 120 deg and to carry out the parametric study and optimization of the liner configuration.

A design of experiment (DOE) approach has been used to build a response-surface model (RSM) of the cost function, i.e., the average OASPL along the downward radiation arc. Successively, the design optimization has been carried through a genetic algorithm (self-adaptive evolution algorithm) applied to the RSM. The corresponding optimal design parameters and liner thickness distribution are reported in Figure 2.

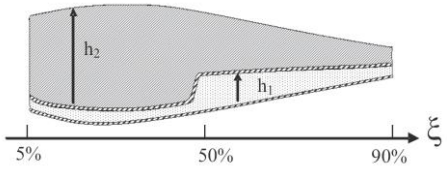

Parameter	Value
Facesheet holes diameter	1.5 mm
Septum holes diameter	0.9 mm
$1-h_2/h$	10%
$1-h_1/h$	36.2%

Figure 2: Schematic representation of the optimal linedflap configuration and optimal design parameters.

The noise reduction accomplished by the optimal linflap configuration is represented by the OASPL contour plots illustrated in Figure 3 that points out a significant noise reduction in the downward direction. The OASPL directivity (Figure 4) shows a noise reduction between 4 and 8 dB along the polar arc with an averaged OASPL of 6.4 dB.

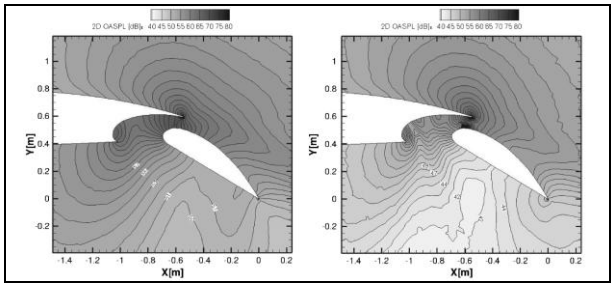

Figure 3: OASPL of the FEM solution. Baseline configuration (left), optimal configuration (right).

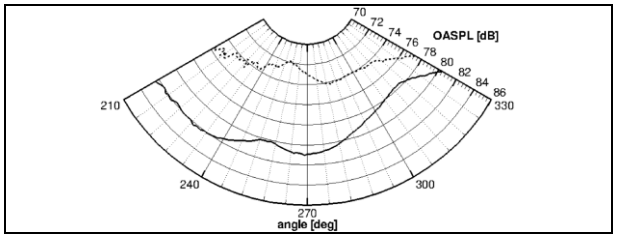

Figure 4: OASPL directivity along the downward radiation arc. Baseline configuration (solid lines), optimal configuration (dashed lines).

III. TF A/C WING SLAT ACOUSTIC LINERS

ONERA has assessed the capabilities of acoustic liners, made of porous materials, to reduce the noise generated by the high lift slats of the regional aircraft configuration with turbofan engines in low speed conditions [8]. The assessment was obtained through aerodynamic and aeroacoustic computations with advanced high fidelity methods: an unsteady ZDES [9][10] method in aerodynamics using the ONERA *elsA* software [11] and a Ffowcs-Williams and Hawkings method for acoustic propagation using the ONERA code *MIA*.

The computations have been performed at Mach number 0.15, angle of attack 9^o and Reynolds number $1.7\ 10^6$.

Figure 5 shows the results of the computation without liner. The Q-criterion isosurface highlights several phenomena. In the slat region, the iso-contours clearly display the spatial location of the free shear layer. A mixing layer is developed from the cusp of the slat in the shear region and borders the main separation bubble on the lower side of the slat. The mixing layer is convected through the slot and more downstream it impacts the lower side of the slat. The figure shows also the large vortices downstream of the slat trailing edge. The pressure fluctuation iso-contours depicts the propagation of concentric waves around the slat.

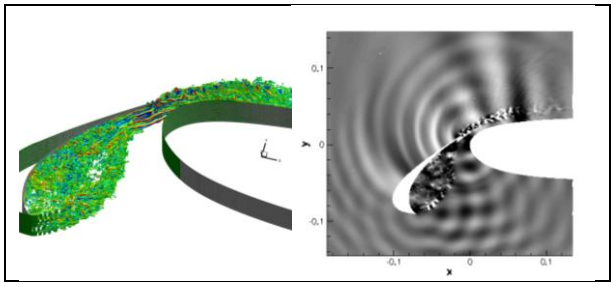

Figure 5: Q-criterion iso-surface (left) and pressure fluctuations iso-contours (right).

The position and the extent of the liner have been selected after a parametric study with the ONERA CAA Euler code *sAbrinA_v0* [12][13] as well as RANS computations with the ONERA *elsA* software. The general Özyörük temporal domain impedance definition was used to take into account within the acoustic computation the absorption effects [14][15] of the liners tested in the ONERA B2A tests [16] which description is reported the *Section VII*.

The analysis of the results carried out by the acoustic parametric study led to the selection of a liner position over a limited region at the slat trailing edge and on a reduced extent at the leading edge of the main body.

For the ZDES computations with liners, the effect of the porous liner was simulated numerically by a specific pressure jump condition on its surface [17].

The far field acoustic results confirm the CFD tendency (Figure 6). A frequency change is observed, due to the acoustical treatment at the trailing edge of the slat since the impedance model acts both on the pressure and tangential flow profiles on the treated walls. The decrease of the acoustical levels is due, on one side to the reduction of the noise sources intensities due to the aerodynamic effect of the liner at the slat trailing edge, and on the other side to the absorbing properties of the treatment on the main body. The SPL highlights a main peak, which can be directly linked to the vortex shedding of the slat trailing edge. Harmonics of this fundamental are also visible. One can also notice that a broadband component is also present in the acoustical pattern.

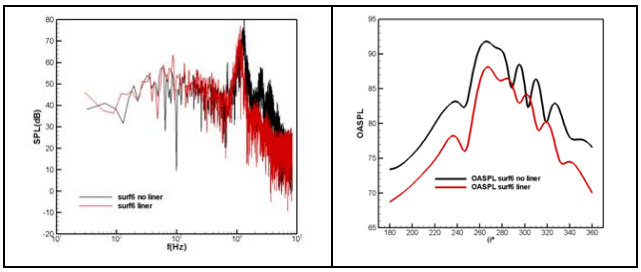

Figure 6: SPL and downward directivity obtained at 90° and 1m from the slat cavity centre.

The overall noise reduction is quite important of about 3 dB and for some angles of observation, the reduction can even reach 5 dB, as can be observed in Figure 6, between the baseline (no liner) and treated (with liner) configurations. Since the acoustical mechanism for this configuration is quite particular, being represented by a highly coherent vortex shedding at the upper trailing edge of the slat, the liner treatment becomes highly efficient. Some less effects are expected when the source changes to a broadband type as it is generally observed in deployed high-lift devices noise.

IV. OR A/C WING FLAP SIDE-EDGE FENCES

One of energetic noise sources of the high lift wing is the turbulent vortex occurring around the flap side-edge. The investigation of the flap side-edge noise was conducted by Chalmers, FOI and CIRA. In this section, a conceptual low-noise fence is presented along with the potential benefits on the noise alleviation.

Two full scale configurations were analysed: the baseline configuration and the fence-on configuration that is formed by attaching a noise-reduction facility onto the baseline configuration. Figure 7 shows the fence-on configuration. The configurations operate at the angle of attack, $\alpha=2^{o}$, and $M_{\infty}=0.2$.

The acoustic assessment has been performed by using a Stochastic Noise Generation and Radiation (SNGR) method [18][19][20] coupled with a Boundary Element Method (BEM) implemented in the commercial software, FINE/Acoustics produced by NUMECA. In the SNGR method, the time-averaged field required comes from a Reynolds-Averaged Navier-Stokes (RANS) computation. In a first step, the kinetic energy and dissipation rate from RANS were processed by the stochastic method to synthetize a turbulent velocity field. According to the Lighthill acoustic analogy, this turbulent field was transformed into the source term of a wave equation and radiated in the frequency space using the BEM.

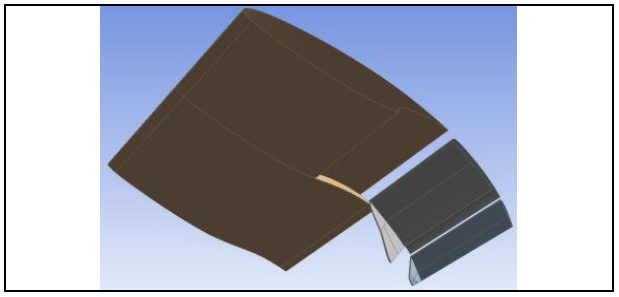

Figure 7: The fence-on configuration.

CIRA provided the RANS solutions that are the inputs for the SNGR method. A computational domain is specified with a span 2.04 m, a height 26 m and a length 26 m. The no-slip condition was applied to the lateral boundaries. The characteristic far-field condition was imposed on the rest of the boundaries. The freestream turbulence intensity was set with a value of 4% and the ratio of the turbulent eddy viscosity and the molecular viscosity is 0.1. The SST k-ω model was used to model the effect of turbulence.

Figure 8 illustrates contours of the RANS-modelled kinetic energy, k_e/U_{∞}^2, in the regions where $k_e/U_{\infty}^2 > 1.1\times10^{-3}$. The regions suggest that the wake of the baseline configuration is of approximately 3 times the chord length. However, the fence results in the wake with 1.5 times the chord length. The highest magnitude in the figure is 0.29 for the baseline configuration and 0.18 for the fence-on configuration.

Therefore, the RANS solutions exhibit that a large amount of energetic turbulences appear near the side edge moving downstream to a long distance and that the fence is an efficient facility to depress the downstream wake reducing significantly noise sources.

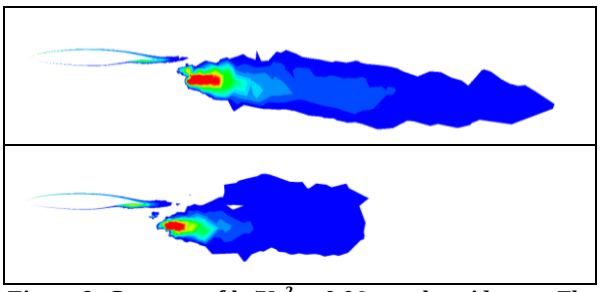

Figure 8: Contours of k_e/U_{∞}^2 at 0.06m to the mid-span. The baseline configuration (top) and the fence-on configuration (bottom). Red represents magnitude above 22×10^{-3}.

Since the noise sources are controlled by the fence, the noise emission was effectively reduced. Figure 9 plots the SPL at the microphone below the configurations and the OASPL at a distance of 500 m. The fence diminishes the noise at the frequencies above 55 Hz, but increases the noise at the rest low frequencies. The OASPL is reduced up to 7 dB.

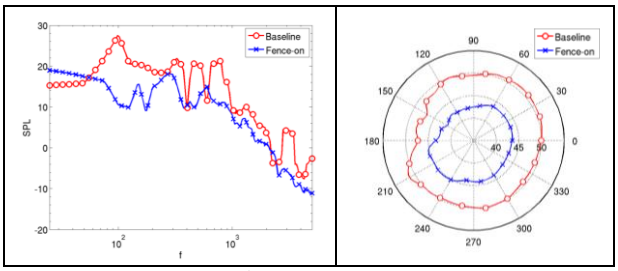

Figure 9: SPL at 270^o and OASPL of the baseline and fence-on configurations

V. TF A/C WING SLAT SETTINGS OPTIMIZATION

A high lift slat noise reduction has been also obtained through a position optimization taking into account aerodynamic and acoustic phenomena. It was carried out by ONERA for the high lift airfoil of the regional aircraft concept with turbofan engines (*Section II*), using an optimization process involving ONERA high-fidelity tools for both CFD and CAA [21]. The optimization problem considered three cost functions to improve: the aerodynamic lift coefficient and the noise level at the same fixed flight condition. However, the objective of a leading-edge device is to improve C_{Lmax} and α_{max} and optimising the slat settings in order to improve C_L at flight conditions could lead to a decrease in maximum lift. Therefore, a third objective function has been considered in order to improve the aerodynamic performance at "high" incidence.

The optimisation approach used in this work was based on surrogate models (SBO), which proceeds by first generating a mathematical model over the complete design space for each cost function using high fidelity methods. During the optimisation process, each surrogate model is enriched with new points located in the region of interest (individual optimum or Pareto of multi-objective optimisation). It can be noted that there is no need to make the high-fidelity evaluation at the same point locations for all the models. For instance, in the present work, some extra points were considered in the aerodynamic model at high angle of attack, due to its "peaky" behaviour in the optimum region, which are not necessary for the acoustic model at flight condition, which is more "regular".

It was observed that the aerodynamic condition at high incidence was preponderant for the optimisation problem that limits the set of Pareto-optimal solutions in the space of design variables, probably because the initial configuration was pre-optimised. Figure 10 compares the initial and the optimized configurations: the most visible change is about the gap and overlap parameters.

Considering the improvement of aero-acoustic performance at flight conditions only leads to a quite different set of solutions, but with a loss in maximum lift. Globally, the following improvements of local performance have been found:

- Increase by 1.2% for C_L at flight conditions;
- Increase by 2.8 % for C_L at high angle of attack;
- Reduction by 70% of local slat noise (in dB) for the 2D wing section (Figure 11).

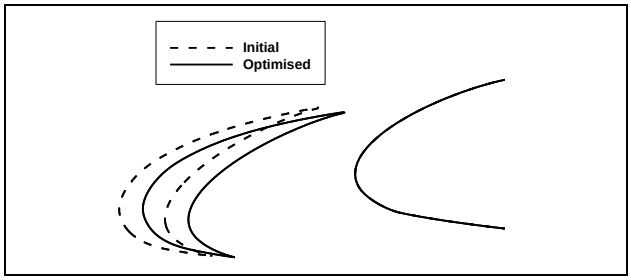

Figure 10: Comparison of initial and optimised configurations.

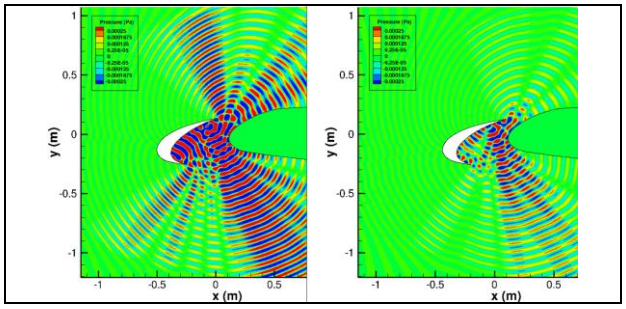

Figure 11: Comparison of computed acoustic fields of initial (left) and optimized (right) configurations.

VI. ASSESSMENT OF TP A/C HIGH-LIFT LOW-NOISE WING CONCEPTS

Aeroacoustic assessment has been performed for conceptual high-lift low-noise wing configurations for a regional aircraft by Chalmers and FOI using an integrated method of acoustic analogies and a hybrid RANS/LES approach [22][23][24][25]. The objective was to explore the noise generation related to the local flow properties. Furthermore, dominant noise sources were recognized for the noise reduction.

The full-scale wing configurations are attached to a common fuselage body for the simulations. Figure 12 shows a 3D view for the baseline configuration and spanwise cut-planes for all the configurations. The baseline configuration consists of a double slotted part-span flap. The wing has a trailing edge kink, and the high-lift system of the flap has separate elements inboard and outboard of the kink. There are cavities for all flaps. Configuration 2 adopts a structure with a single slotted part-span flap. Configuration 3 is formed by adding a Krueger flap to Configuration 2. The Mach

number of the freestream flow is 0.2, and the Reynolds number is 1.7×10^7.

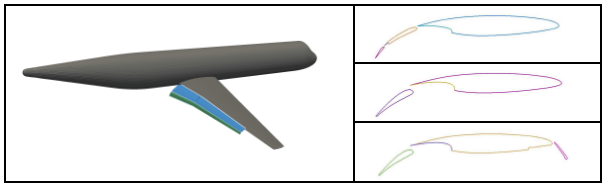

Figure 12: A 3D view for the baseline configuration, and span-wise cuts for, from top to bottom, the Configuration 1 (baseline), Configuration 2 and Configuration 3.

Turbulence-resolving simulations was made by the CFD solver Edge [26][27]. A precursor computation of vorticity was done using RANS, to determine a suitable position for an integral surface that is needed by the acoustic analogies. The grids were then generated in line with topology of the integral surface.

The aerodynamic investigation shows that Configuration 4 with the Krueger flap performs best on the lift generation. Although the efficiency (C_L/C_D) is slightly lower than the other configurations, the maximum lift is almost 20% higher. The Krueger flap leads to flow separation on the inboard flap. On the other hand, the other configurations show the flow separation on the outboard flaps. An energetic noise source is the vortex induced by the kink between the inboard and outboard flaps, as displayed in Figure 13.

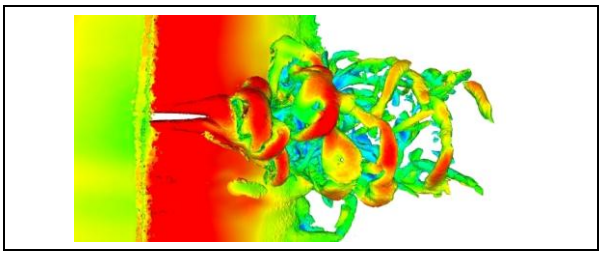

Figure 13: Isosurface of vorticity magnitude $\|\omega\|$ = 1000, coloured by velocitiy magnitude $\|U\|$ where red means large value.

The noise in far-field was predicted using the acoustic analogies: the Kirchhoff method [28], the FW-H method of the permeable surface [29] and the Curle method [30] by assuming a uniform medium at rest. The turbulence-resolving data were used as inputs for the acoustic analogy methods. The Kirchhoff method and FW-H method are valid to predict the total noise since the integral surface defined for them encloses all the potential noise sources. The pressure fluctuation on the wall is used for the Curle method.

Configuration 3 highlighted the best acoustic performance. The Krueger flap that is installed onto this configuration is effective to depress the flow separation on the main wing and the vortices at the kink. Meanwhile, the noise induced by the Krueger flap is negligible.

Figure 14 compares the configurations in terms of the SPL and OASPL at a distance of 500 m computed with the FW-H method. The OSAPL of the noise produced by Configuration 4 is 6-10 dB lower than that by the other configurations.

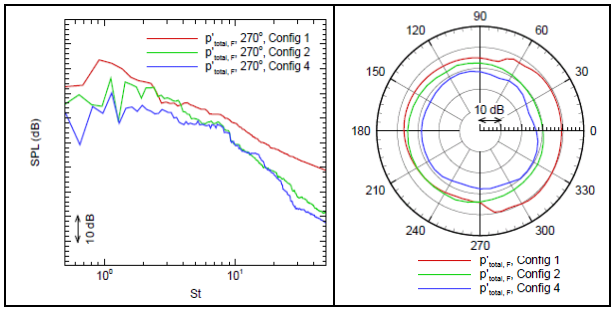

Figure 14: SPL and OASPL of Configuration 1 (baseline), Configuration 2 and Configuration 3.

VII. EXPERIMENTAL CHARACTERISATION OF ACOUSTIC LINERS FOR HIGH-LIFT LOW-NOISE DEVICES.

Acoustic liners of different types, with perforated plates and honeycomb (SDOF) and with two stages of resonators (2DOF), have been manufactured by Fraunhofer and INCAS then characterised in the ONERA aeroacoustic test bench B2A, in presence of incident acoustic waves and grazing flow [16] (Figure 15). The aim was to supply an experimental database for further computations relative to High-Lift Devices Low Noise treatments (*Section II*). In addition to the classical technique based on microphone measurements for the determination of the liner characteristics, a new 2D Laser Doppler Velocimetry technique has been applied, giving a detailed description of the acoustic field.

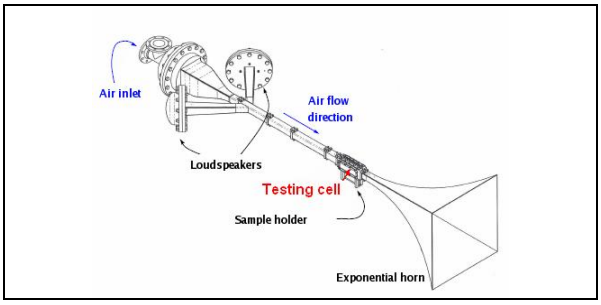

Figure 15: Schematic view of the Onera test bench B2A.

The tests have shown that, for liners with local reaction, the area of influence of the liner is relatively independent from the external mean flow [16].

The acoustic specific impedance has been assessed by the classical technique (Figure 16): the outcome was that the tested liners cover a wide range of impedance that satisfies the requirements of the project for HLD low noise treatments, that is to say a specific resistance $0.2 < R/\rho c < 1.5$ and a specific reactance $-4 < X/\rho c < 1$ between 1 and 4 kHz.

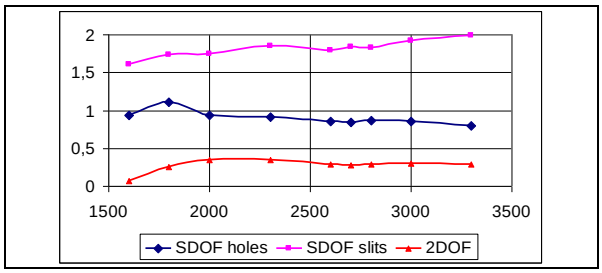

Figure 16: Evolution of liners resistance with frequency.

VIII. WT INVESTIGATIONS OF HIGH-LIFT LOW-NOISE CONFIGURATIONS

An experimental campaign was carried out at the INCAS Subsonic Wind Tunnel in order to characterize the aero-acoustic performance of different trailing edge High Lift Devices, mounting noise reducing systems in both Turbo Prop (TP) and Open Rotor (OR) wing configurations. The models were manufactured and instrumented by INCAS under the supervision of CIRA and Alenia.

The test program involved three different side-edge fences of different shapes, a Kruger slat device and the lined flap. Further experimental investigations, not included in the present work, were also performed on morphing flaps. Aeroacoustic results, evaluated by either classical pressure measurements or beamforming techniques, were compared with the baseline flap in order to investigate and quantify the potential aeroacoustic benefits.

An under floor balance was used during experiments to quickly position models in both pitch and yaw axis over a large angles range. Furthermore, due to the high loads expected in the test campaign for GRA TP and OR models, an external mounting system was designed, manufactured and installed in the tunnel. This system allowed to provide enhanced testing capabilities at high angle of attack and high speeds, by minimizing, at the same time, any spurious noise contribution to the acoustic field produced by the devices during the tests.

In order to evaluate the capability and the level of confidence in the experimental data captured in operative conditions, tests were repeated at different velocities. For the baseline test cases, where loads were below the maximum Lift capability of the balance, the global loads were measured using the balance. This was mainly the case for base configuration at V1, and for some limited cases in other configurations at V2. For the remaining configurations, lift was also computed by integrating the experimental pressure distributions captured on the wing profile. Noise measurements were carried out by a dedicated setup consisting of a circular array of 72 microphones distributed over an hard foam panel placed on the ceiling of the test section. The microphones array, having 1 meter of diameter, contained also a videocamera in the middle of the circle enabling very fast localization of noise sources. The signals measured by the microphones were sent to a dedicated data acquisition system managed by a personal computer via ethernet gigabit connection. After recording, the data were processed by a commercial software implementing the beamforming algorithm for source identification and acoustic "maps". In addition, Fourier analyses were off-line performed.

In order to correlate aeroacoustic performance with actual aerodynamic conditions, a significant number of Kulite (XCS-062) sensors were installed inside the flaps (up to 29 on the sigle flap configuration), near the tip (fences region). The Kulite signals were recorded by a secondary data acquisition system.

A pre-test activity took place under supervision of CIRA. It was dedicated to the assessment of the benefits associated with a series of noise reducing improvements developed for the testing facility. The background noise and aeolian tones from one and two tandem placed rods benchmarks were assessed before and after applying noise absorbing panels to the side walls and rear to the test chamber (Figure 17).

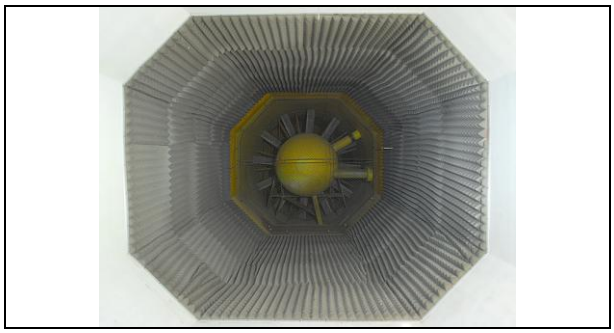

Figure 17: Noise absorbing material in the front of the engine.

Also small scale adaptations were applied and further background noise measurements were carried out. Another important aspect taken into consideration was the capability of the beam-forming technique to localize several punctual sources in the wind tunnel environment using a microphone array. This refinement activity performed on the Wind Tunnel facility resulted in a positive reduction of the background noise without any device installed higher than 3 dB on a relevant frequency interval. This made possible the detection of lower intensity noise sources from the models tested inside the wind tunnel.

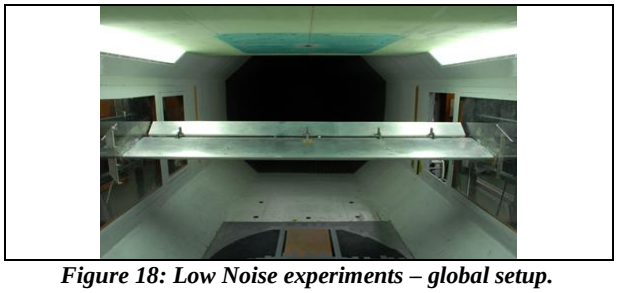

Figure 18: Low Noise experiments – global setup.

During the WT aeroacoustic tests, the struts of the balance were removed and the model was installed upside down in order to allow the array of microphones to measure noise from the pressure side (Figure 18).
The distance from the center of the microphones array to the model was 0.78 m. Acoustic data from the array microphones were simultaneously measured at a sample frequency of 96 kHz and a measurement time of 8 s. In parallel Kulite signals were measured by a dedicated data aquisition system using 40 kHz sampling frequency. The test measurements were performed for different model configurations, at different flow speeds. The obtained noise spectra, as well as the noise sources were successfully identified. An extensive set of digital acoustic images were obtained and compared with the baseline configurations.

For the TP configuration with single slotted flap, the lined-flap concept (Figure 19) was evaluated.
A lined-flap model was manufactured by INCAS following the requirements given by CIRA and Alenia. Experimental results confirmed the potential of this innovative low-noise solutions in reducing the aerocoustic emission of the treated flap region. The effectiveness of this technology was evaluated by beamforming images (Figure 20) showing a good agreement with the numerical predictions (*Section I*).

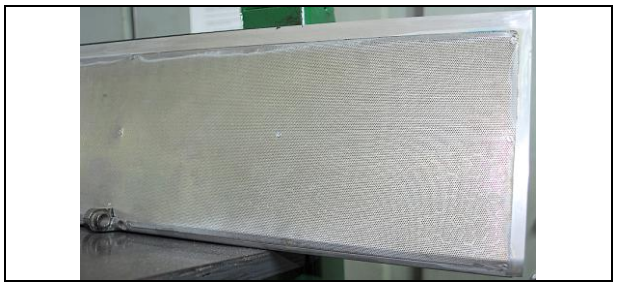

Figure 19: Linedflap model used in the experimental campaign.

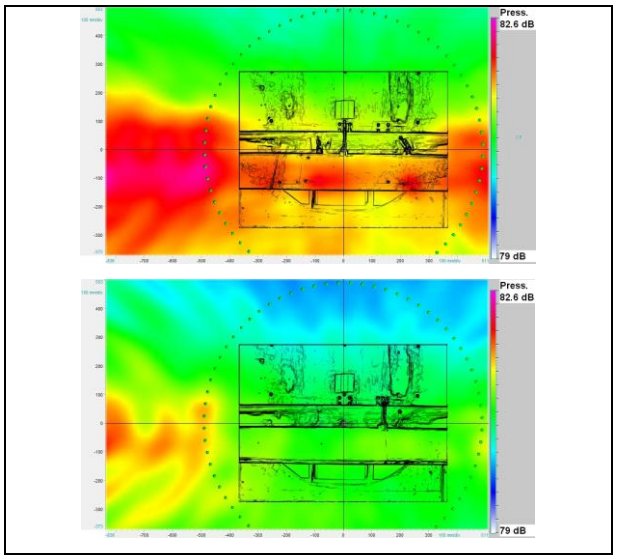

Figure 20: Beamforming results comparison– Without liner (top)/With liner (bottom).

Several side-edge fences were also tested for the TP single slotted flap (Figure 21) and the OR double slotted flap.

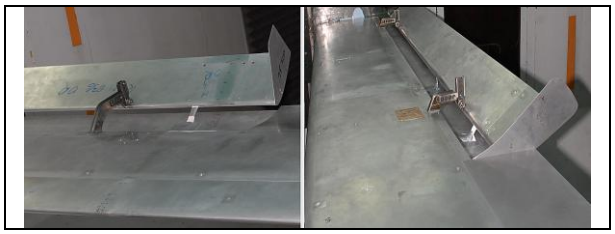

Figure 21: Several types of fences for the TP single slotted flap.

Figure 22 shows the beamforming results for the OR double-slotted flap. The noise sources visualization, generated by means of beamforming, is shown at a frequency of about 3.2 kHz by focusing on the flap side-edge for a free stream velocity of 45 m/s and an angle of attack of 6 degrees. As numerically assessed, the acoustic benefits of the fence device are clearly highlighted in terms of source strength reduction near the flap side-edge (*Section III*).

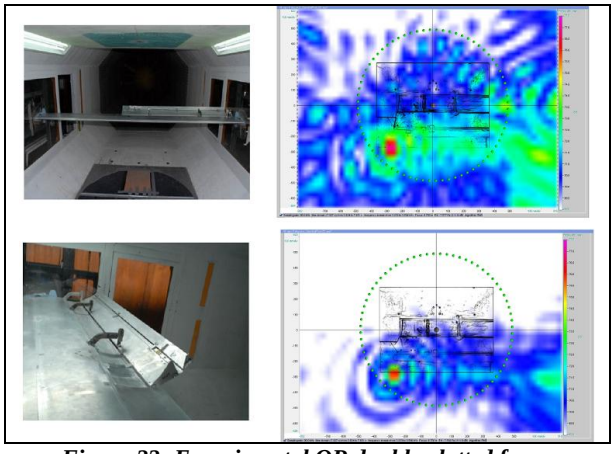

Figure 22: Experimental OR double-slotted fence results:Comparison between baseline (top) and fence device (bottom).

A Kruger slat device located upstream the clean OR wing with single-slotted flap was also evaluated. Comparing the “clean” single-slotted flap spectrum with the one generated by the installed Krueger, a reasonable agreement is achieved up to 10 kHz whereas a noise tone can be distinguished at higher frequencies from the broadband noise generated by the “clean” single-slotted flap configuration (Figure 23). This tone reflects the vortex shedding phenomenon generated by the Krueger blunted trailing-edge whose suppression might be achieved through a careful trailing edge shape design.

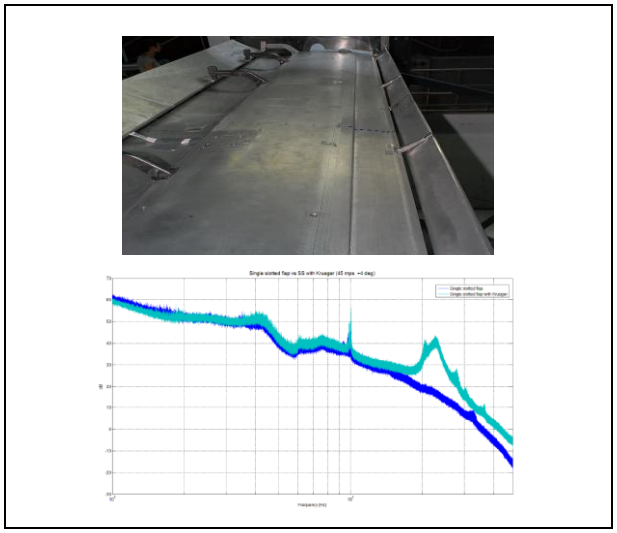

Figure 23: OR single slotted flap with Kruger slat (top). Comparison between baseline and Kruger (bottom).

IX. CONCLUSIONS

Technological studies of High-Lift Low-Noise devices carried out in the framework of the GRA ITD project have been presented.

Both computational analyses and wind tunnel tests have been described in detail.

Some passive acoustic devices have been firstly analyzed with different numerical approaches. First of all, the use of conventional liners, as acoustic treatments carefully integrated with the wing, have revealed to be effective in noise reuction for a wide range of frequencies. Also side-edge fences have demonstrated a promising aptitude in suppression of the turbulent vortex occurring around the flap side-edge. These encouraging results have been also confirmed during an extensive WT test campaign.

Finally, multiobjective optimizations and the numerical assessment of several configurations have been performed by applying both aerodynamic and aeroacoustic methodologies. These studies have showed the successfully design of high lift technologies with a low noise impact.

The most promising among the addressed HLD technologies will be brought to the final demonstration phase within the GRA ITD work programme, in order to assess in a realistic experimental environment (TRL 5) the aircraft low-speed aerodynamic and aero-acoustic performances through WT tests on large-scale (say 1:6) complete A/C powered models.

REFERENCES

[1] D. Casalino, M. Barbarino: " Optimization of a Single-Slotted Lined Flap for Wing Trailing-Edge Noise Reduction" Journal of Aircraft, Vol. 49, No. 4, pp 1051-1063, 2012. DOI 10.2514/1.C031561.

[2] R. Ewert, C. Appel, J. Dierke, and M. Herr, "RANS/CAA Based Prediction of NACA 0012 Broadband Trailing Edge Noise and Experimental Validation," AIAA Paper 2009-3269, May 2009.

[3] Casalino, D., "Finite Element Solutions of a Third-Order Wave Equation for Sound Propagation in Sheared Flows," AIAA Paper 2010- 3762, June 2010.

[4] Casper, J., and Farassat, F., "Broadband Trailing Edge Noise Predictions in the Time Domain," Journal of Sound and Vibration, Vol. 271, Nos. 1–2, 2004, pp. 159–176. DOI 10.1016/S0022-460X(03)00367-5.

[5] Myers, M. K., "On the Acoustic Boundary Condition in the Presence of Flow," Journal of Sound and Vibration, Vol. 71, No. 3, 1980, pp. 429–434.DOI10.1016/0022-460X(80)90424-1.

[6] Motsinger, R. E., and Kraft, R. E., "Design and Performance of Duct Acoustic Treatment," Aeroacoustics of Flight Vehicles: Theory and Practice, Volume 2: Noise Control, edited by H. H. Hubbard, NASA Langley Research Center, Hampton, VA, 1991, pp. 165–206.

[7] Optimus, Software Package, Ver. 5.2, Noesis Solutions, Leuven, Belgium, 2006.

[8] S, Ben Khelil, T. Le Garrec, D.-C. Mincu: "TF A/C Wing LE Slat Acoustic Liners Design - Generic Airfoil Studies." JTI-GRA O2.2.1-07, July 2012.

[9] Deck S., "Recent improvements in the Zonal Detached Eddy Simulation (ZDES) formulation", Theor. Comput. Fluid Dyn. Vol. 26, No. 6, pp 523-550, 2012. DOI 10.1007/s00162-011-0240-z.

[10] Deck, S., and Laraufie, R., "Numerical investigation of the flow dynamics past a three-element aerofoil", J. Fluid Mech. (2013), vol. 732, pp. 401-444. © Cambridge University Press 2013. doi:10.1017/jfm.2013.363.

[11] Cambier, L., Heib, S., and Plot, S., "The Onera elsA CFD software: input from research and feedback from industry", Mechanics & Industry 14, 159–174 (2013). © AFM, EDP Sciences 2013 DOI:10.1051/meca/2013056 www.mechanics-industry.org.

[12] Redonnet S., Manoha E. and Sagaut P, Numerical Simulation of Propagation of Small Perturbations Interacting with Flows and Solid Bodies, AIAA Paper n° 2001-2223, 7th CEAS/AIAA Aeroacoustics Conference, Maastricht, The Netherlands, 28-30 May, 2001.

[13] Terracol, M., Manoha, E., Herrero, C., Labourasse, E., Redonnet, S. and Sagaut, P., Hybrid Methods for Airframe Noise Numerical Prediction, Theoretical and Computational Fluid Dynamics, Vol. 19, No.3, July 2005.

[14] Delattre, G., Sagaut, P., Manoha, E. and Redonnet, S., Time-domain Simulation of Sound Absorption on Curved Wall, 13th AIAA/CEAS Aeroacoustics Conference.

[15] Ozyoruk, Y. and Long, L.N., A Time-domain Implementation of Surface Acoustic Impedance Condition with and without Flow, AIAA and CEAS, Aeroacoustics Conference, 2nd, State College, PA, May 6-8, 1996.

[16] F. Simon: "HLD Acoustic Liners Experimental Characterization: Description, Test Report and Results Analysis." JTI-GRA D2.2.1-04, November 2012.

[17] M. R. Khorrami, M.M. Choudhari, Application of Passive Porous Treatment to Slat Training Edge Noise. NASA/TM-2003-212416.

[18] W. Béchara, C. Bailly, P. Lafon and S. Candel, "Stochastic approach to noise modeling for free turbulent flows," AIAA Journal, 32(3):455–464, 1994.

[19] M. Billson, L.-E. Eriksson and L. Davidson, "Jet noise modeling using synthetic anisotropic turbulence," AIAA Paper 2004-3028, 2004.

[20] D. Casalino and M. Barbarino, "A stochastic method for airfoil self-noise computation in frequency-domain," AIAA Paper 2010-3884, 2010.

[21] F. Moëns, D. Bailly, Th. Le Garrec, D-C Mincu: "ATF A/C Wing HLD Multi-Disciplinary Optimisation." JTI-GRA D2.2.1-15, September 2013.

[22] H.-D. Yao, L. Davidson, L.-E. Eriksson, S.-H Peng, O. Grundestam and P. E. Eliasson, "Surface Integral Analogy Approaches for Predicting Noise from 3D High-Lift Low-Noise Wings," Acta Mechanica Sinica, 2014, DOI:10.1007/s10409-014-0008-y.

[23] O. Grundestam, S.-H Peng, P. E. Eliasson, H.-D. Yao, L. Davidson and L.-E. Eriksson, "Local Flow properties in relation to noise generation for low-noise high-lift configurations", AIAA paper 2012-278, 2012.

[24] P. E. Eliasson, O. Grundestam, S.-H Peng, H.-D. Yao, L. Davidson and L.-E. Eriksson, "Assessment of high-lift concepts for a regional aircraft in the ALONOCO project", AIAA paper 2012-277, 2012.

[25] H.-D. Yao, L.-E. Eriksson, L. Davidson, S.-H Peng, O. Grundestam and P. E. Eliasson, "Aeroacoustic Assessment of Conceptual Low-Noise High-Lift Wing Configurations," AIAA paper 2012-383, 2012.

[26] S.-H. Peng, "Algebraic Hybrid RANS-LES modelling applied to incompressible and compressible turbulent flows," AIAA paper 2674-2690, 2006.

[27] P. Eliasson, "Edge, a Navier-Stokes Solver for Unstructured Grids," Proceedings to Finite Volumes for Complex Applications III, pp. 527-534, 2002.

[28] A.S. Lyrintzis, "Review: the Use of Kirchhoff Method in Computational Aeroacoustics," ASME Journal of Fluids Engineering, 116 (4), pp. 665-676, 1994.

[29] K.S. Brentner and F. Farassat, "An Analytical Comparison of the Acoustic Analogy and Kirchhoff Formulation for Moving Surfaces," AIAA Journal, 36 (8), pp. 1379-1386, 1998.

[30] N. Curle, "The Influence of Solid Boundaries upon Aerodynamic Sound," Proc. Roy. Soc. A, 231, pp. 505-514, 1955.